Earth Surface Processes and Landforms
Earth Surf. Process. Landforms **27**, 1285–1297 (2002)
Published online 26 September 2002 in Wiley InterScience (www.interscience.wiley.com). DOI: 10.1002/esp.409

AN INTEGRATED HYDROLOGICAL MODEL FOR RAIN-INDUCED LANDSLIDE PREDICTION

P. L. WILKINSON,[1] M. G. ANDERSON[2]* AND D. M. LLOYD[1]

[1] *ZNA (UK) Ltd, First Floor, University Gate, Park Row, Bristol, UK*
[2] *Department of Geographical Sciences, University of Bristol, University Road, Bristol, UK*

Received 14 May 2001; Revised 18 April 2002; Accepted 31 May 2002

ABSTRACT

This paper describes an extension to the Combined Hydrology And Stability Model (CHASM) to fully include the effects of vegetation and slope plan topography on slope stability. The resultant physically based numerical model is designed to be applied to site-specific slopes in which a detailed assessment of unsaturated and saturated hydrology is required in relation to vegetation, topography and slope stability. Applications are made to the Hawke's Bay region in New Zealand where shallow-seated instability is strongly associated with spatial and temporal trends in vegetation cover types, and the Mid-Levels region in Hong Kong, an area subject to a variety of landslide mechanisms, some of which may be subject to strong topographic control. An improved understanding of process mechanism, afforded by the model, is critical for reliable and appropriate design of slope stabilization and remedial measures. Copyright © 2002 John Wiley & Sons, Ltd.

KEY WORDS: rainfall; vegetation; slope hydrology; stability analysis; numerical modelling

INTRODUCTION

This paper outlines an integrated hydrological model for slope stability analysis. Whilst there have been considerable recent advances in terms of geotechnical modelling (Griffiths and Lane, 1999), there remains a critical need to establish models that fully integrate hydrological process controls on slope stability. Hydrological controls such as hillslope soil-water convergence and vegetation cover have direct impacts on pore pressure conditions and hence slope stability (Montgomery and Dietrich, 1994; Greenway *et al*., 1987). These factors reflect complex two- and three-dimensional aspects of soil-water movement within the slope mass and provide important dynamic pore-pressure boundary conditions at the slope surface which impact on slope stability.

At present there is no available slope stability model that fully incorporates and combines the resultant effects on dynamic (temporally changing) pore pressure of slope plan topographic form and vegetation interaction. The principal aim of this paper is therefore to develop a high-resolution fully integrated hydrological model capable of investigating spatially and temporally complex slope stability analysis. Such an integrated approach to slope stability modelling and analysis is a prerequisite for the correct identification of dominant slope stability process controls.

CURRENT MODELLING APPROACHES

Common techniques used in geotechnical engineering for the assessment of slope stability are Bishop's (1955) simplified circular method and Janbu's (1954) non-circular method. These limit equilibrium methods are used to determine the shear stress along the failure surface, the mobilized shear strength, and the ratio between these two, the factor of safety (FOS), providing a measure of the relative stability of the slope (Nash (1987) provides a major review of limit equilibrium methods of analysis). Pore pressures along a slip surface may

* Correspondence to: M. G. Anderson, Department of Geographical Sciences, University of Bristol, University Road, Bristol, BS8 1SS, UK. E-mail: m.g.anderson@bristol.ac.uk

be incorporated in a number of ways, although hydrostatic conditions (i.e. definition of a hydrostatic phreatic surface, r_u, or static piezometric pressure) are often assumed in preference to incorporating full hydrodynamic computations.

Like dSLAM (distributed Shallow Landslide Analysis Model; Wu and Sidle, 1995), CHASM (Combined Hydrology And Stability Model) allows assessment of the effects of three-dimensional form and vegetation on slope stability. However, CHASM operates at a scale consistent with standard engineering slope stability analysis and therefore places the spatial resolution on slope-specific cross-sections, as opposed to topographic plan (dSLAM integrates GIS-driven topography into an infinite slope stability analysis). Additionally, CHASM allows direct investigation into the hydrological effects associated with vegetation, such as interception and evapotranspiration, and their resultant effect on slope stability.

DEVELOPING AN INTEGRATED HYDROLOGICAL MODEL FOR SLOPE STABILITY

The procedure adopted to model the hydrological system is a forward explicit finite difference scheme, in which the slope is divided into a series of rectangular columns, each subdivided into regular cells (see Figure 1; cell centre point computational nodes are shown). The model simulates detention storage, infiltration, evaporation, and unsaturated and saturated flow regimes. More specifically, rainfall is allowed to infiltrate the top cells at a rate governed by the infiltration capacity. Unsaturated vertical flow through each column

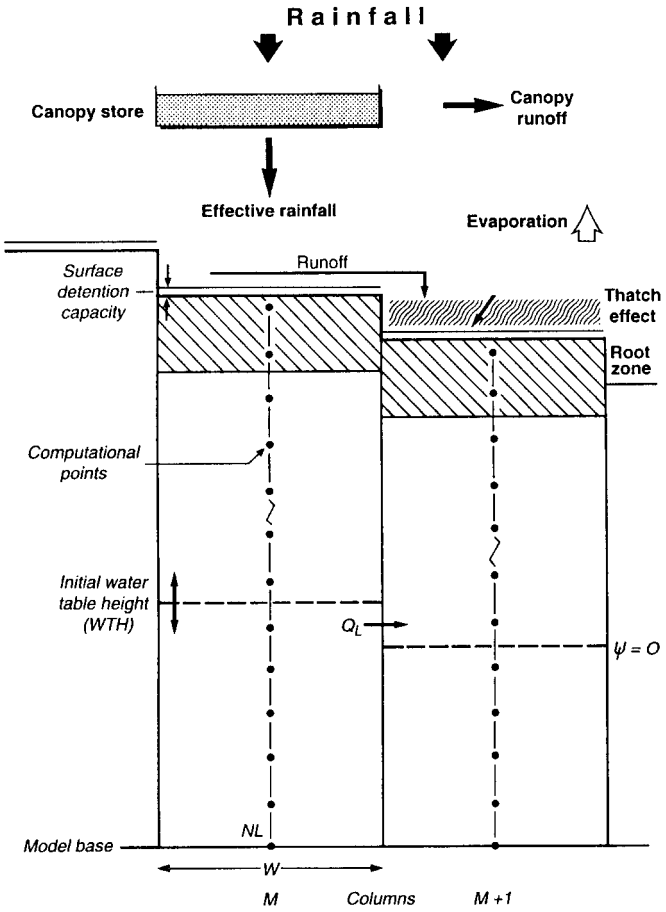

Figure 1. Finite difference model scheme: ψ, matric suction (m), Q_L, lateral flux (m s^{-1}), W, column width (m), M, column number; NL, vertical node spacing (m)

is computed using Richards' (1931) equation solved in explicit form (Equation 1), with the unsaturated conductivity being defined by the Millington–Quirk (1959) procedure:

$$\frac{\partial\theta}{\partial t} = -\frac{\partial}{\partial z}\left(K\frac{\partial\psi}{\partial z}\right) - \frac{\partial K}{dz} \tag{1}$$

where θ is the volumetric moisture content ($m^3\ m^{-3}$), dt is the time step (s), z represents the vertical depth (m), K is the vertical unsaturated hydraulic conductivity ($m\ s^{-1}$) and ψ is the matric suction (m) (negative pore-water pressure). Flow between columns is modelled using the Darcy (1856) equation for saturated flow. As is usual in such finite difference formulations, unsaturated flow is assumed to take place only in the vertical direction (see for Marshall and Holmes, 1979, p. 94). At each major time step of the simulation the hydrology module is directly coupled to a limit equilibrium method for determining slope stability. In the model formulation outlined here, pore pressures, both negative and positive, are incorporated directly into the effective stress determination of the Mohr–Coulomb equation for soil shear strength:

$$s = c' + (\sigma - u)\tan\phi' \tag{2}$$

where s is the soil shear strength ($kN\ m^{-2}$), c' is the effective soil cohesion ($kN\ m^{-2}$), ϕ' is the effective angle of internal friction (degrees), σ is the total stress acting normal to the slip surface ($kN\ m^{-2}$), u represents pore-water pressure (both positive and negative, kPa). This approach, though a simplification, approximates that used by Fredlund *et al*., (1978) to incorporate the effects of negative pore pressures on slope stability in the range 0–10 kPa.

Whilst the scheme has the facility to incorporate the full Fredlund *et al*. (1978) formulation, Equation 2 does provide a sound approximation in the 0–10 kPa range (due to uncertainty in the estimation of ϕ^b, the angle of internal friction with respect to matrix suction, and the requirements for very precise experimental control (Anderson and Kemp, 1987; Lloyd 1990)).

The three-dimensional topographic nature of slopes has been ignored with respect to pore-pressure impacts. However, slope failure often occurs in areas of convergent topography where subsurface soil water flowpaths give rise to excess pore-water pressures downslope (Anderson *et al*., 1988). Failure to reflect, in some way, this three-dimensional impact on both total and soil-water potentials is likely to result in an over-estimation of the slope factor of safety. In the integrated model structure developed here, slope plan curvature (convexity and concavity) is represented by variable column breadth, with the stability computation being made in two dimensions in the downslope direction. Computational node consistency is thereby maintained for both the hydrological and geotechnical determinations. The soil-water flux computation is effectively treated in the same manner as the two-dimensional scheme described above. However, downslope saturated fluxes are enhanced (slope plan convergence) or reduced (slope plan divergence) in accordance with the downslope cell breadth changes specified. This formulation is designed to be consistent with two-dimensional stability analyses, in that the model is not distributed in the third dimension in terms of hydrological properties, but is capable of reflecting the process of soil-water convergence and divergence. Additionally, it is geometrically consistent with the slope plan index measure provided by the Hong Kong Geotechnical Control Office (1980).

It is equally necessary to reflect the upper boundary conditions of the slope in terms of hydrological behaviour, in that surface cover can have a significant impact on both the hydrological and geotechnical aspects of slope stability. Surface cover effects can be complex in terms of both achieving sufficiently detailed process representation and appropriate parameterization. Vegetation affects slope hydrology and slope stability through the three principal hydrological mechanisms of interception, root water uptake and evapotranspiration, as well as through changes to the soil saturated hydraulic conductivity (Wu *et al*. 1979; Greenway *et al*., 1987). In addition to this there are also mechanical vegetation effects in the form of root reinforcement and added surcharge. The model structure outlined below is designed to reflect these complex interactions (Figure 2).

Interception of precipitation depends on the type of vegetation. For example, dense stands of tall grass can be flattened by intense rainfall to form a semi-permeable barrier. (Lamb and Premchitt (1990) showed from experimental plots in Hong Kong that between half and three-quarters of all rain formed runoff without the

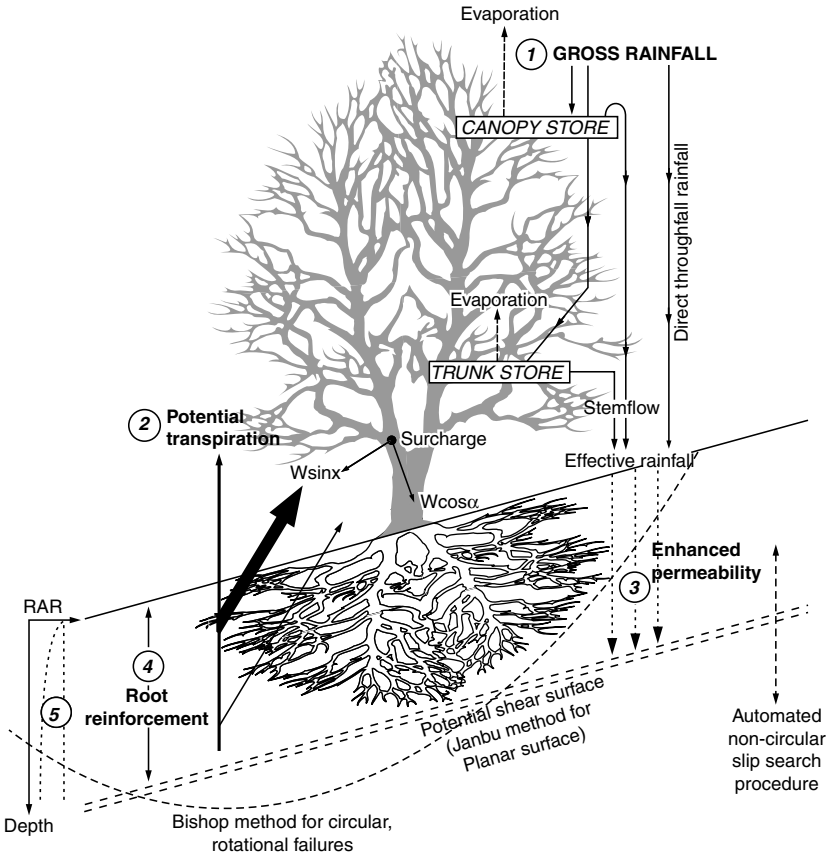

Figure 2. Vegetation–slope interactions. 1, Rutter model (Rutter *et al*., 1971); 2, Penman–Monteith (Monteith, 1973); 3, permeability model (Collison, 1993); 4, root reinforcement (Wu *et al*., 1979); 5, water uptake model (Feddes *et al*., 1976), where RAR is the root-area ratio

infiltration capacity of the soil having been reached). For a grass cover, this process is modelled by reducing the hourly rainfall intensity applied to the surface of the slope, according to grass depth. For interception by trees, canopy structure is described by the free throughfall coefficient (p), the stemflow-partitioning coefficient (p_t), the canopy storage capacity (S) and the trunk storage capacity (S_t) (Rutter *et al*., 1971; Valente *et al*., 1997). The model estimates throughfall, stemflow and interception loss from input rainfall and meteorological data, based on the dynamic calculation of the water balance through the equations:

$$(1 - p - p_t) \int R dt = \int D dt + \int E dt + \Delta C \tag{3a}$$

$$p_t \int R dt = S_f + \int E_t dt + \Delta C_t \tag{3b}$$

where R is the intensity of gross rainfall (m s^{-1}), D is the rate of drainage from the canopy (m s^{-1}), E is the evaporation rate of water intercepted by the canopy (m s^{-1}), ΔC is the change in canopy storage (m), S_f is the stemflow (m), E_t is the evaporation rate of the water intercepted by the trunks (m s^{-1}) and ΔC_t is the change in the trunk storage (m). The free throughfall coefficient, p, is a function of the canopy cover and ranges from 0 (no canopy cover) to 1 (complete canopy cover), and thus determines the appropriate partitioning of precipitation between direct ground surface input and input into the Rutter interception model. Evaporation from a saturated canopy is calculated using the Penman–Monteith equation with the canopy

resistance (r_c) set to zero, since leaf stomata close under saturated conditions and the process of transpiration is halted (Wilkinson *et al.*, 1998).

$$E_p = \frac{\Delta R_n + \rho c_p VPD/r_a}{\lambda[\Delta + \gamma(1 + r_c/r_a)]} \tag{4}$$

In Equation 4, E_p is the potential evapotranspiration rate (m s^{-1}), r_a and r_c are the aerodynamic and canopy resistances, respectively (s m^{-1}), Δ is the slope of the saturation vapour pressure-temperature curve (kg m^{-3} K^{-1}), *VPD* represents the vapour pressure deficit (kg m^{-1} s^{-2}), c_p is the specific heat of air (J kg^{-1} K^{-1}), and R_n represents the net radiation (W m^{-2}). It is assumed in the model that evaporation from the trunk and canopy stores occurs at the same rate.

The second hydrological mechanism relates to evapotranspiration and root water uptake. The extraction of moisture from the soil via the root network and loss of water from the leaf surface result in reduced pore-water pressures within the slope (Hoogland *et al.*, 1981; Lafolie *et al.*, 1993), potentially leading to increased effective shear strengths and increased slope stability. Factors such as type, size and species of vegetation, climatic and seasonal factors, and features of the growing site must all be considered for an accurate representation of evapotranspiration rates and the associated effect on slope stability. To determine the magnitude of this effect, the Penman–Monteith (Monteith, 1973) equation for evapotranspiration is adopted (Equation 4, with the inclusion of a canopy resistance term, r_c). This is coupled with the spatial distribution of the roots and the soil moisture content to determine the rate of water uptake from each portion of the soil (Wilkinson *et al.*, 1998). To link the transpiration rates to actual root water uptake, the hourly transpiration values are converted to metres per second according to the leaf-area index and density of water:

$$T_v = \left(\frac{T}{\rho_w}\right) LAI \tag{5}$$

where T is the transpiration flux density (kg m^{-2} s^{-1}), T_v is the transpiration rate (m s^{-1}), ρ_w is the density of water (kg m^{-3}) and *LAI* represents the leaf-area index (m^2 m^{-2}). To calculate the amount of moisture removed from the soil, the rate of transpiration is distributed throughout the depth of the roots, providing variation in water extraction with depth according to the rooting density. The maximum rate of water uptake, assuming a homogeneous root distribution (Feddes *et al.*, 1976) is as follows:

$$S_{\max} = T_v/z_r \tag{6}$$

where $S_{\max}$ = maximum uptake rate (m s^{-1}) and z_r is the root depth (m). Under non-optimal conditions (i.e. either too dry or too wet) $S_{\max}$ is reduced by means of a pressure-head-dependent α-function:

$$S(h) = \alpha(h) S_{\max} \tag{7}$$

where $S(h)$ is the actual root water uptake (m s^{-1}) and $\alpha(h)$ is a dimensionless factor based on the pressure head, h (Feddes *et al.*, 1976). Water uptake below $|h_1|$ (oxygen deficiency) and above $|h_4|$ (wilting point) is set equal to zero. Between $|h_1|$ and $|h_2|$ a linear variation is assumed. This is also the case for pressure heads between $|h_3|$ and $|h_4|$. At each iteration time step, the computed water uptake term for all cells containing roots ($S(h)$, Equation 7) acts as a sink term in Richards' equation (Equation 1). The final hydrological effect is concerned with the increase in soil hydraulic conductivity as a result of the root network. The magnitude of this effect is well documented and can be determined by an equation relating the root-area ratio to the saturated hydraulic conductivity:

$$\Delta K_s = \alpha + \beta RAR \tag{8}$$

where ΔK_s is the increase in saturated hydraulic conductivity (m s^{-1}), α and β are constants, and *RAR* is the root-area ratio (%) (see Collison, 1993; Collison *et al.*, 1995).

In addition to the hydrological effects, vegetation has a geotechnical impact on slope stability through the mechanical effects of root reinforcement and vegetation surcharge. The interaction between roots and soil can be quantified using a simple perpendicular root model (Wu *et al*., 1979; Wu and Sidle, 1995). This considers roots as elements initially crossing a slip plane perpendicularly. The effect of shear displacement on elastic vertical roots crossing the shear zone is to increase the confining stress and direct shear resistance along the failure plane at the onset of shear. The mobilization of the tensile resistance of roots in vegetated soils can be modelled as an increase in c (denoted as c_R), the total cohesion of the soil:

$$\Delta c = c_R = t_R(\cos\theta \tan\phi + \sin\theta) \tag{9}$$

where θ is the angle of shear rotation (degrees), ϕ is the angle of internal friction (degrees) and t_R represents the average tensile strength of the roots or fibres per unit area of soil (kN m^2):

$$t_R = T_R(A_R/A) \tag{10}$$

Here, T_R is the average tensile strength of root or fibre (kN m^{-2}) and A_R/A is the root-area ratio (m^2 m^{-2}). Schiechtl (1980) provides a comprehensive review of root tensile strengths for a range of trees, shrubs and grasses (see also Abernethy and Rutherford, 2001). The only unknown in Equation 9, θ, varies with thickness of the shear zone and the amount of shear displacement. Field observations by Wu *et al*. (1979) indicate that this value varies between 45° and 70°. In situations where very detailed parameterization data are available, the shearing resistance and, therefore, the contribution of root reinforcement to the effective cohesion can be represented by root depth distributions, root system morphology and root pullout resistance (e.g. Riestenberg, 1994).

The effect of the final mechanical component, vegetation surcharge, depends on the stress–strain properties of the slope material, soil permeability, slope geometry, and in particular the presence or absence of cohesion (Greenway *et al*., 1987). Gray and Megahan (1981), for instance, showed that surcharge would be beneficial when cohesion is low, groundwater level is high and slope angles are relatively small compared to the friction angle of the material. In order to model the effects of surcharge, the weight of the vegetation on the slope surface is distributed through the soil profile according to the vertical and horizontal distance from the source of loading, and added appropriately to the overall weight of the slice.

The vegetation model described above is implemented within the scheme using the Janbu (1954) non-circular limit equilibrium technique. The normal force acting perpendicular to the slice base, P_v, is calculated as follows:

$$P_v = \left[(W + S_w) - \frac{1}{FOS}((c' + c'_R)l \sin\alpha - ((u - u_v)l)\tan\phi' \sin\alpha)\right] / m_\alpha \tag{11}$$

where

$$m_\alpha = \cos\alpha + \frac{\sin\alpha \tan\phi'}{FOS} \tag{12}$$

In Equation 11, vegetation surcharge is represented by S_w (kPa), u_v represents the combined effects of interception, evapotranspiration and increased permeability (kPa) and c_R is the additional cohesion derived from root reinforcement (kPa). The term u, pore-water pressure, is derived from the hydrological model scheme with the inclusion of variable plan topography. In addition, l represents the length of the slice base (m), W is the slice weight (kPa) and α is the slice angle (degrees). The final FOS is expressed as:

$$FOS = \frac{\sum_{i=0}^{n} ((c' + c'_R)l + (P_v - (u - u_v)l)\tan\phi')\sec\alpha}{\sum_{i=0}^{n} (W + S_w)\tan\alpha} \tag{13}$$

Equation 13 is determined on each hour of the simulation using the numerical schemes for slope plan topography, vegetation interaction and the unsaturated and saturated hydrodynamics. To complement the enhanced slope hydrological representation afforded by the incorporation of these model components, it is appropriate to develop a non-circular slip search procedure as part of the slope stability determination. Traditionally, engineering approaches have approximated the shear surface as circular. Although this method may be used to search for the most critical slip surface, which defines a range of the centres of rotation via a grid search technique, failures are often non-circular due to hydrological and geotechnical discontinuities within the slope profile (Waldron and Dakessian, 1981; Brooks *et al*., 1993). To assess these non-circular failures an engineer typically defines the position of the slip surface. In cases where the failure plane is known (e.g. back analysis of an existing failure with an exposed failure surface) this approach may be viable. However, where the most critical slip surface is unknown, assuming a single position for the slip surface is clearly inadequate. Furthermore, a manual search for the critical failure surface is time-consuming and potentially inaccurate. Accordingly, it is appropriate to incorporate an automated non-circular slip surface routine within the model structure. This is especially the case for vegetated slopes where imposed hydrological and geotechnical variability in soil properties may produce complex slip surfaces.

The unique element of the procedure adopted here, unlike previous search algorithms based on hydrostatic conditions (Jade and Shanker, 1995; Shanker and Mohan, 1987), is that it employs hydrodynamic pore-pressure conditions. The numerical method is based on a search technique for finding the global minima of a constrained non-linear optimization problem. Initially, the feasible search domain is defined according to an upper and lower bound defined by the user, and slip surfaces are generated within the specified domain. The FOS is then calculated for each slip surface according to the Janbu limit equilibrium technique (Equation 13) and then optimized via quadratic interpolation to determine the most critical non-circular slip surface, according to the prevailing hydrological and geotechnical controls. Wilkinson *et al*. (2000), in outlining the full analytical basis of the scheme, have shown that implementation of such an automated slip search leads to an improvement in the evaluation for stability conditions compared with less rigorous methods. The resultant integrated hydrological model, incorporating the effects of vegetation, slope plan topography and a non-circular slip method for stability analysis, is shown schematically in Figure 3.

DISCUSSION OF NUMERICAL RESULTS

The integrated model developments allow investigation of scenarios that hitherto have not been possible due to the inherent process representation limitations of existing models. Two case studies are provided as examples. The first illustrates the importance of surface cover in relation to two-dimensional slope stability dynamics and is based on the Hawke's Bay region of the east coast of the North Island, New Zealand. The second illustration incorporates convergent slope plan curvature chosen to demonstrate the relation of hillslope soil-water convergence on resultant pore pressures and slope stability, with differing cover conditions, for the Mid-Levels region of Hong Kong. In both cases the fully automated non-circular slip surface is employed.

Hawkes Bay, New Zealand

Over recent years commercial plantations have become widespread as a component of the forestry industry throughout the North Island of New Zealand. The management of this land with regard to cutting procedures has been shown to have a significant impact on slope stability (Sidle, 1992, 1999) and therefore it is of interest to further investigate the relationship between vegetation and landslide activity. To this effect the vegetation model described in this paper can now be applied to a scenario comparing the stability of a slope covered with Radiata pine with a slope cleared of vegetation (i.e. bare slope with no vegetation effects). Radiata pine has been the subject of in-depth studies with detailed examination of both above- and below-ground biomass characteristics (O'Loughlin and Watson, 1979; Watson and O'Loughlin, 1990); this information enables full parameterization of the vegetation model outlined above (Table I). A typical slope configuration is shown in Figure 4a.

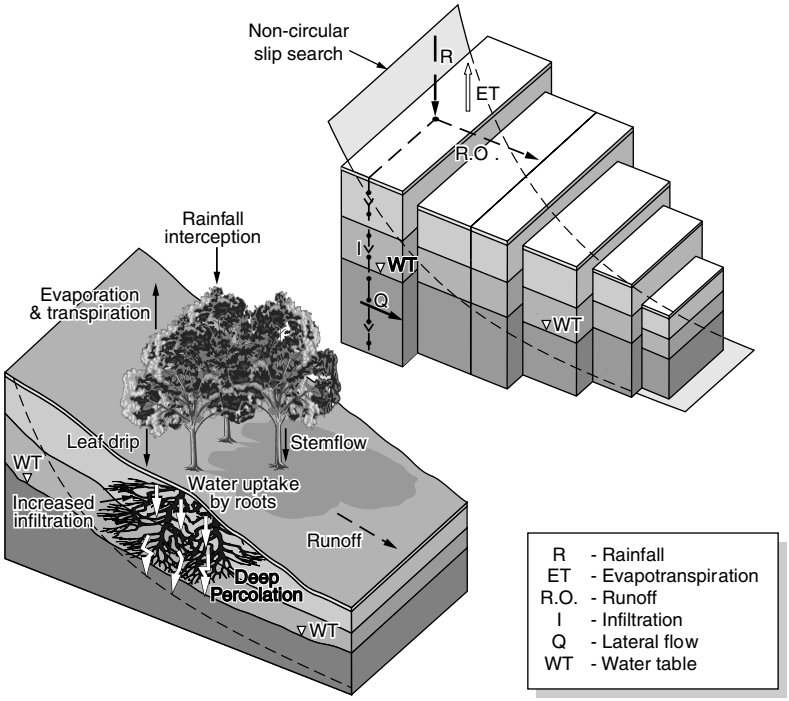

Figure 3. Representation of the integrated hydrology slope stability model

Table I. Model input parameters for Radiata pine

Variable	Radiata pine
Root tensile strength (kN m^{-2})	17
RAR (m^2 m^{-2})	0·1
Ground cover (%)	20
Spacing (m)	2
Lateral root extent (m)	4
Vertical root depth (m)	2
Surcharge (kN m^{-2})	3
LAI (m^2 m^{-2})	16
Canopy resistance (s m^{-1})	100
Aerodynamic resistance (s m^{-1})	10

A one-in-2-years, 24 h design storm event was simulated following a 24 h period of simulation without precipitation (total simulation time = 48 h, rainfall intensity = 10 mm h^{-1}). In this example, the upslope left-hand boundary condition was treated as a zero flux boundary, thereby allowing focus on the vegetation–slope interactions and removing the need to model a potential upslope catchment area. However, if required, appropriate upslope fluxes can be applied to the left-hand boundary to represent upslope contribution to groundwater flow. The top boundary condition is set in accordance with the rainfall event with the infiltration capacity being governed by the unsaturated hydraulic conductivity achieved after running the model without rain for the first 24 h of the simulation.

During the period of precipitation the non-vegetated slope fails when positive pore-water pressures develop along the soil–bedrock interface with the formation of a perched water table (an average pore-water pressure of 3 kPa along the slip surface with failure occurring 14 h into the simulation at hour 38, after 144·2 mm of

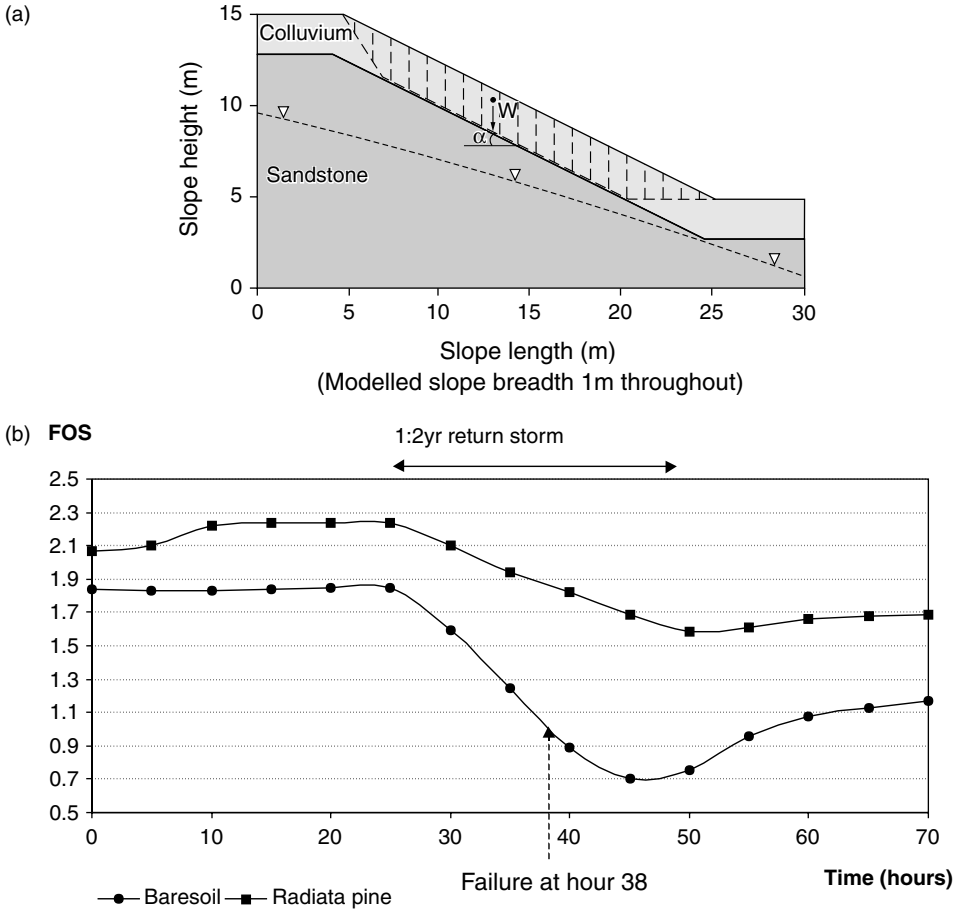

Figure 4. (a) Slope form and associated soil hydrological and geotechnical properties for Hawke's Bay, New Zealand, scenario (colluvium: $c' = 1$ 4kPa, $\phi' = 18°$, $K_s = 4{\cdot}17 \times 10^{-5}$ m s^{-1}; sandstone: $c' = 5$ kPa, $\phi' = 35°$, $K_s = 1{\cdot}03 \times 10^{-6}$ m s^{-1}), includes automated non-circular critical slip location and illustrative slices (W = total slice weight (kN), α = angle at base of slice (degrees)). (b) Surface cover effects on slope stability: a comparison between bare soil and Radiata pine covers in terms of FOS change during a one-in-2-year storm event

precipitation has fallen). The non-circular failure surface associated with the minimum FOS was located at an average depth of 75–100 cm below the surface of the slope, above the soil–bedrock interface.

By contrast, with a vegetated slope cover comprising Radiata pine, effective shear strength is enhanced through the processes of transpiration, root water uptake and root network reinforcement. The modelled processes of interception and evapotranspiration under Radiata pine combine to maintain soil suction above the critical threshold for slope stability. In this case the minimum FOS attained was 1·59 (Figure 4b). In fact, for such a vegetated slope a storm event of 280 mm in 24 h was required for slope failure to occur. Such a storm has a return period of approximately 9 years; correlating well with historical evidence (Marden and Rowan, 1993; Blaschke *et al.*, 1992).

A comparison between measured and model-predicted volumetric moisture contents in response to a three-day, medium-intensity storm event (total rainfall = 179·3 mm) in the Hawke's Bay region has provided basic validation of the hydrology component of the model. At depths of 25 cm and 100 cm the model-predicted changes in the volumetric moisture content to within 10 per cent of the measured values (for a pasture-covered slope; Wilkinson, 2000). Although this type of validation is limited in both spatial and temporal terms it does provide some initial indication that the process of infiltration and downward percolation towards the soil–bedrock interface is being represented in a realistic manner.

Further investigations into the relationship between vegetation cover and landslide occurrence (total length of landslide scars and landslide density associated with pasture, scrub, pine and indigenous vegetation covers) have provided support to model results by allowing comparison on the basis of threshold landslide-triggering rainfall events and associated probability of landslide occurrence with observed temporal trends (Blaschke *et al*., 1992; Marden and Rowan, 1993; Hicks *et al*., 1993).

Comparisons to such historical datasets provide a useful means of assessing the overall performance of the model as opposed to rigorous internal validation of individual model components and associated process representation.

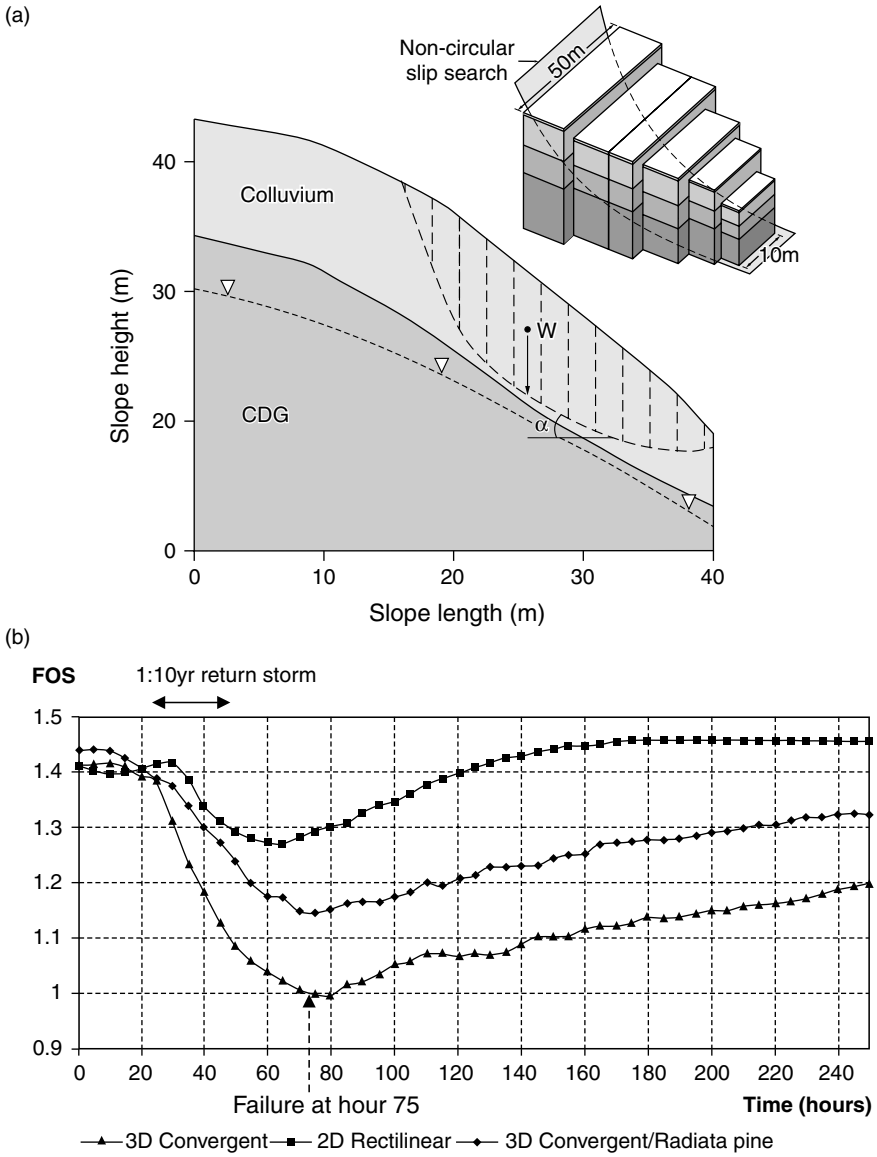

Figure 5. (a) Slope form and associated soil hydrological and geotechnical properties for Hong Kong scenario (colluvium: $c' = 4$ kPa, $\phi' = 39^\circ$, $K_s = 2 \times 10^{-5}$ m s^{-1}; CDG = completely decomposed granite: $c' = 6$ kPa, $\phi' = 37^\circ$, $K_s = 1 \times 10^{-6}$ m s^{-1}), includes automated non-circular critical slip location and illustrative slices (W = total slice weight (kN), α = angle at base of slice (degrees)). (b) Topographical effects on slope stability for bare surface two- and three-dimensional convergent and vegetated three-dimensional convergent scenarios for a one-in-10-year, 24 hour return period storm in Hong Kong

Application of the integrated vegetation–slope model to the Hawke's Bay region has highlighted the importance of model process representation. The numerical results have illustrated that omitting vegetation-related processes (root water uptake, interception and root reinforcement) in such a sensitive area could result in a miscalculation of the FOS and misrepresentation of the dominant process controls on stability.

Mid-Levels, Hong Kong

Inclusion of surface cover effects can be complemented by a consideration of plan topographical form effects on the pore pressure regime. In tropical residual soils the importance of sub-surface hydrology as a landslide-triggering mechanism has been thoroughly investigated over the last 20 years (Fredlund *et al*., 1978; Anderson *et al*., 1988; Anderson and Kemp, 1991). In terms of dimensionality there are circumstances where topography and its effect on the conveyance of both surface and sub-surface flows will influence slope stability. In this case the standard two-dimensional approach is insufficient, typically leading to over-estimation of the factor of safety in areas of plan convergence.

The second illustration provided is based on conditions typical of the Mid-Levels area of Hong Kong. Here steeply vegetated slopes, residual soils and complex plan topography provide an ideal context for illustrating the factor of safety differentials that can result from hydrological controls on slope stability. Figure 5 shows the results of applying the scheme using a one-in-10-year 24 h storm to the slope profile given in Figure 5a. The slope plan convergence modelled had an upslope breadth of 50 m reducing to 10 m at the downslope toe location; as such the slope plan curvature corresponds to category C1 in the slope plan curvature classification used by the Hong Kong Geotechnical Control Office *CHASE Report* (1980).

Analysis of the convergent slope with a bare soil cover yields a minimum factor of safety of 0·98, corresponding to a near-circular failure surface. This figure increases to 1·15 when the slope has a vegetated cover (of Radiata pine) and further to 1·28 when the effect of slope plan convergence is removed (i.e. a two-dimensional planar slope, retaining the vegetated cover). These scenarios provide important evidence of the need to develop slope stability models that integrate relevant hydrological processes. Clearly, amongst the benefits of such a modelling scheme is the fact that inter-comparisons of different vegetation effects on slope stability processes can be made.

CONCLUSIONS

Previous stability models have been limited in terms of the hydrological processes they include and yet such processes can have significant impacts upon both negative and positive pore-water pressures. This paper has presented a model that seeks to develop these process-based inclusions. Incorporation of variable plan topography combined with surface cover has been shown to significantly affect the predicted rainfall threshold required for slope failure. Such a finding has profound implications on the identification of the resultant processes that control slope stability and, importantly, on slope design and specification of remedial and stabilization measures. The further development of integrated hydrology–stability models is therefore considered a major avenue of research that needs to be pursued.

ACKNOWLEDGEMENT

The authors acknowledge the comments provided by Professor David Muir-Wood in the preparation of this paper.

REFERENCES

Abernethy B, Rutherford ID. 2001. The distribution and strength of riparian tree roots in relation to riverbank reinforcement. *Hydrological Processes* **15**: 63–79.

Anderson MG, Kemp MJ. 1987. Suction-controlled triaxial testing: laboratory procedures in relation to resistance envelope methods. *Earth Surface Processes and Landforms* **12**: 649–654.

Anderson MG, Kemp MJ. 1991. Towards an improved specification of slope hydrology in the analysis of slope instability problems in the tropics. *Progress in Physical Geography* **15**(1): 29–52.

Anderson MG, Kemp MJ, Lloyd DM. 1988. Applications of soil water finite difference models to slope stability problems. *Proceedings of the 5th International Symposium on Landslides*, Vol. 1., Lausanne, 10–15 July 1988. 525–530.
Bishop AW. 1955. The use of the slip circle in the stability analysis of slopes. *Geotechnique* **5**(1): 7–77.
Blaschke PM, Trustrum NA, DeRose RC. 1992. Ecosystem processes and sustainable land use in New Zealand steeplands. *Agriculture, Ecosystems and Environment* **41**: 153–178.
Brooks SM, Richards KS, Anderson MG. 1993. Shallow failure mechanisms during the Holocene: utilisation of a coupled slope hydrology – slope stability model. In *Landscape Sensitivity*, Thomas D, Allison R (eds). John Wiley and Sons: Chichester; 149–175.
Collison AJC. 1993. *Assessing the influence of vegetation on slope stability in the tropics*. Ph.D. Thesis, University of Bristol.
Collison AJC, Anderson MG, Lloyd DM. 1995. Impact of vegetation on slope stability in a humid tropical environment: a modelling approach. *Proceedings of the Institute Civil Engineers, Water Maritime & Energy* **112**: 168–175.
Darcy H. 1856. *Les Fontaines Publique de la Ville de Dijon*. Dalmont: Paris.
Feddes RA, Kowalik P, Kolinska-Malinka K, Zaradny H. 1976. Simulation of field water uptake by plants using a soil water dependent root extraction functions. *Journal of Hydrology* **31**: 13–26.
Fredlund DG, Morgernstern NR, Widger RA. 1978. Shear strength of unsaturated soils. *Canadian Geotechnical Journal* **15**: 313–321.
Gray DH, Megahan WF. 1981. *Forest vegetation removal and slope stability in the Idaho Batholith*. USDA Forest Service Research Paper INT-271.
Greenway DR, Anderson MG, Brian-Boys KC. 1987. Vegetation and slope stability. In *Slope Stability*, Anderson MG, Richards KS (eds). Wiley: Chichester; 187–230.
Griffiths DV, Lane PA. 1999. Slope stability analysis by finite elements. *Geotechnique* **49**(3): 387–403.
Hicks DL, Fletcher JR, Eyles GO, McPhail CR, Watson M. 1993. *Erosion of hill country in the Manawatu-Wanganui region 1992: Impacts and options for sustainable land use*. Landcare Research Contract Report LC9394/51.
Hong Kong Geotechnical Control Office. 1980. *CHASE report*, Volume 1: Appendix G.
Hoogland JC, Feddes RA, Belmans C. 1981. Root water uptake model depending on soil water pressure head and maximum extraction rate. *Acta Horticulturae* **119**: 123–136.
Jade S, Shanker KD. 1995. Modelling of slope failure using a global optimisation technique. *Engineering Optimisation* **23**: 258–266.
Janbu N. 1954. Application of composite slip surface for stability analysis. *Proceedings of the European Conference on the Stability of Earth Slopes*, Vol. 3, Stockholm. 43–49.
Lafolie F, Bruckler L, Tardieu F. 1993. Modelling root water potential and soil-water transport: I. Model presentation. *Soil Science Society of America Journal* **55**: 1203–1212.
Lamb TSK, Premchitt J. 1990. *Rainfall–runoff on slopes 1984–1988*. Civil Engineering Services Report Hong Kong. Special Project Report I 1/90.
Lloyd DM. 1990. *Modelling the hydrology and stability of tropical cut slopes*. PhD Thesis, University of Bristol.
Marden M, Rowan D. 1993. Protective value of vegetation on tertiary terrain before and during Cyclone Bola, East Coast, North Island, New Zealand. *New Zealand Journal of Forestry Science* **23**(3): 255–263.
Marshall TJ, Holmes JW. 1979. *Soil Physics*. Cambridge University Press: Cambridge.
Millington RJ, Quirk JP. 1959. Permeability of porous media. *Nature* **183**: 387–388.
Monteith JL. 1973. *Principles of Environmental Physics*. Edward Arnold: London.
Montgomery DR, Dietrich WE. 1994. A physically based model for the topographic control on shallow landsliding. *Water Resources Research* **30**: 1153–1171.
Nash DFT. 1987. A comparative review of limit equilibrium methods of slope stability. In *Slope Stability: Geotechnical Engineering and Geomorphology*, Anderson MG, Richards KS (eds). Wiley: Chichester; 11–75.
O'Loughlin CL, Watson A. 1979. Root wood strength deterioration in radiata pine after clearfelling. *New Zealand Journal of Forestry Science* **9**: 284–293.
Richards LA. 1931. Capillary conduction of liquids in porous mediums. *Physics* **1**: 318–333.
Riestenberg MM. 1994. *Anchouring of thin colluvium by roots of sugar maple and white ash on hillsides in Cincinnati*, US Geological Survey Bulletin 2059-E.
Rutter AJ, Kershaw KA, Robins PC. 1971. A predictive model of rainfall interception in forests. I. Derivation of the model from observation in a plantation of corsican pine. *Agricultural Meteorology* **9**: 367–384.
Schiechtl HM. 1980. *Bioengineering for Land Reclamation and Conservation*. University of Alberta Press: Edmonton, Canada.
Shanker K, Mohan C. 1987. A random search technique for the global minima of constrained non-linear optimization problems. *International Conference on Optimization Techniques and Applications*, Singapore, 8–10 April 1987. IEEE; New York; 905–918.
Sidle RC. 1992. A theoretical model of the effects of timber harvesting on slope stability. *Water Resources Research* **28**: 1897–1910.
Sidle RC. 1999. Simulating effects of timber harvesting on the temporal and spatial distribution of shallow landslides. *Zeitschrift fur Geomorphologie* **43**(2): 185–201.
Trustrum NA, Page MJ. 1992. The long-term erosion history of Lake Tutira watershed: implications for sustainable land use management. In *Proceedings of the International Conference on Sustainable Land Management*, Henriques PR (ed.). 212–215.
Valente F, David JS, Gash JHC. 1997. Modelling interception loss for two sparse eucalypt and pine forests in central Portugal using reformulated Rutter and Gash analytical models. *Journal of Hydrology* **190**: 141–162.
Waldron LJ, Dakessian S. 1981. Soil reinforcement by roots: calculation of increased soil resistance from root properties. *Soil Science* **132**: 427–434.
Watson AJ, O'Loughlin CL. 1990. Structural root morphology and biomass of three age classes of Pinus radiata. *New Zealand Journal of Forestry Science* **20**(1): 97–110.
Wilkinson PL. 2000. *Investigating the hydrological and geotechnical effects of vegetation on slope stability: development of a fully integrated numerical model*. PhD Thesis, University of Bristol.
Wilkinson PL, Brooks SM, Anderson MG. 1998. Investigating the effect of moisture extraction by vegetation upon slope stability: further developments of a combined hydrology and stability model (CHASM). *British Hydrological Society International Symposium on Hydrology in a Changing Environment*. *Theme 4*: *Hydrology of environmental hazards*, Exeter. 165–178.

Wilkinson PL, Brooks SM, Anderson MG. 2000. Design and application of an automated non-circular slip surface search within a combined hydrology and stability model (CHASM). *Hydrological Processes* **14**: 2003–2017.
Wu W, Sidle RC. 1995. A distributed slope stability model for steep forested basins. *Water Resources Research* **31**: 2097–2110.
Wu TH, McKinnell WP III, Swanston DN. 1979. Strength of tree roots and landslides on Prince of Wales Island, Alaska. *Canadian Geotechnical Journal* **16**(1): 19–33.

